PUBLICATIONS OF THE ASTRONOMICAL SOCIETY OF THE PACIFIC, 112:237–250, 2000 February

V893 Scorpii: The Brightest Eclipsing Cataclysmic Variable below the Period Gap[1]

ALBERT BRUCH, J. E. STEINER, AND C. D. GNEIDING
Laboratório Nacional de Astrofísica, C.P. 21, CEP 37500-000, Itajubá, MG, Brazil; albert@lna.br

Received 1999 September 11; accepted 1999 November 8

ABSTRACT. We report about the first time-resolved photometric observations of the bright dwarf nova V893 Sco. The optical light curves show eclipses recurring with a period of 01:49:23 which are probably caused mainly by the hot spot while the accretion disk center with the white dwarf remains uneclipsed. The light curves show considerable cycle-to-cycle variations concerning the mean magnitude, the strength of the orbital hump, the presence of an intermediate hump, and the amplitude and minimum depth of the eclipses. Light curves in the J and H bands are essentially constant without ellipsoidal variations of the secondary star. Surprisingly there is no sign of an eclipse at these wavelengths. V893 Sco exhibits a strong flickering activity with statistical properties which are remarkably stable when compared to other cataclysmic variables. The short timescale flickering ($<0.01P_{\rm orb}$) is not confined to the accretion disk but contains a contribution from the hot spot. During one night an oscillation with a period of 5.71 ± 0.02 minutes was observed. A beat with the orbital period may also be present. A spectrum taken in the range of Hβ shows the double-peaked Balmer emission typical for high-inclination dwarf novae and permits one to predict the presence of a strong S-wave in time-resolved spectroscopy, consistent with the prominent orbital hump in the light curves. The oscillations, the properties of the flickering, the presence of He II emission, and the hard X-rays seen by *ROSAT* suggest a connection of V893 Sco to intermediate polars, but there is not yet conclusive evidence for such a classification.

1. INTRODUCTION

Cataclysmic variables (CVs) are well known to be short-period interacting binary systems where a Roche lobe filling main-sequence star (except for some rare systems containing a somewhat evolved body), the secondary, transfers matter via an accretion disk to a white dwarf primary.

The structure of CVs can best be studied in systems where the secondary, which is faint and contributes in most cases only negligibly to the optical light, eclipses periodically the bright accretion disk and the white dwarf during its orbital revolution. In such systems it is possible not only to derive the orbital period easily and accurately but also to set more stringent limits on many system parameters such as the orbital inclination, the mass ratio of the components, and—in favorable cases—the individual masses than is possible in noneclipsing systems. Moreover, eclipses are of paramount importance for the observational study of the structure of accretions disks, an issue of importance beyond CVs because disks are common in many astrophysical environments as diverse as newly forming stars and active galactic nuclei. The detection of eclipses in CVs is therefore always an important event, in particular if the system is bright and can be studied in detail with modest instrumental efforts.

Here we report about the discovery of eclipses in V893 Sco. This system was identified as a variable star and classified as a dwarf nova by Satyvoldiev (1972). However, it got lost thereafter. Only recently, Kato et al. (1998) reidentified V893 Sco. Having been lost for a quarter of a century, no detailed observations of the star have ever been published. Our knowledge of V893 Sco is basically restricted to a long-term light curve shown by Satyvoldiev (1982) and the magnitude ($V = 13.0$) and color ($B-V = 1.0$) published by Petrov & Satyvoldiev (1975). Furthermore, V893 Sco can be identified with the *ROSAT* All Sky Survey source 1RXS J161516.2−283712. When this paper was almost completed, we got notice of a short publication of Thorstensen (1999), who presents some spectroscopic observations.

In the present contribution the first time-resolved photometry of V893 Sco is described. It led to the detection of eclipses recurring with a period of 01:49:23, making V893 Sco the brightest eclipsing CV below the gap in the CV period distribution and one of the brightest such systems in the overall CV population.

2. OBSERVATIONS

Observations of V893 Sco were carried out on several occasions in 1999 May and June, using the facilities of the

[1] Based on data collected at CNPq/Laboratório Nacional de Astrofísica, Brazil.

Observatório do Pico dos Dias, Laboratório Nacional de Astrofísica, Brazil. A complete summary of the observations is given in Table 1.

Differential CCD photometry using a thin back-illuminated EEV-CCD as detector was performed on May 4 and 5 at the 0.6 m Boller & Chivens and the 0.6 m Zeiss telescopes using standard V and R (Cape system) filters. The light curves obtained in these exploratory observations were of relatively short duration and low time resolution. Nevertheless, both of them clearly showed an eclipse which stimulated us to perform further photometry, using the same detector, but now in a high time resolution mode. These observations were taken in white light with the exception of June 11/12 when a $CuSO_4$ filter (transmitting basically the blue and ultraviolet light) as defined by Bessell (1990) was used.

Additionally, infrared light curves of V893 Sco were obtained on 1999, May 31/June 1 (J band) and June 1/2 (H band) at the 0.6 m Boller & Chivens telescope using the CamIV, an infrared camera which contains a 1024 × 1024 pixel HAWAII HgCdTe detector, operated at a temperature of 77 K. The projection scale was $\approx 0\farcs95$ pixel^{-1}.

Two spectra in the range of Hβ (4650–5540 Å) were exposed on 1999 June 2 (courtesy João Francisco Santos, Jr.), using a Cassegrain spectrograph attached to the 1.6 m telescope.

The basic reductions of the data were performed using IRAF. This includes debiasing and flat-fielding, as well as optimized extraction and wavelength calibration of the spectroscopic observations. Light curves were constructed from the direct images using the IRAF script LCURVE (courtesy Marcos P. Diaz) which makes use of DAOPHOT/APPHOT routines. An aperture size 2.2 times the FWHM of the stellar images was chosen for the optical as well as for the IR photometry. On an absolute scale it varied according to the seeing conditions. A typical value of the FWHM was 2″–2.″5. Since the field of V893 Sco is not crowded—the nearest (faint) visible neighbor is at a distance of ≈30″—source confusion does not play a role. Four stars in the vicinity of V893 Sco were used as comparison stars. The further analysis of the data was done using the MIRA software system (Bruch 1993).

3. EPHEMERIS

The optical light curves (shown in Fig. 2 and discussed in detail in § 4.1) are characterized by eclipses which enable a measurement of the orbital period of V893 Sco and the derivation of an ephemeris. It is in general not possible to identify unequivocally the ingress or egress of the white dwarf in the eclipse profiles of V893 Sco as, e.g., in the cases of OY Car (Vogt et al. 1981) or Z Cha (Bailey 1979). Therefore, we cannot exactly define the epochs of the conjunction between the red and the white dwarfs. All we can do is to determine the epochs of the eclipse centers. As will be shown in § 4.1, the minima are largely due to eclipses of the hot spot and only to a minor degree of the accretion disk.

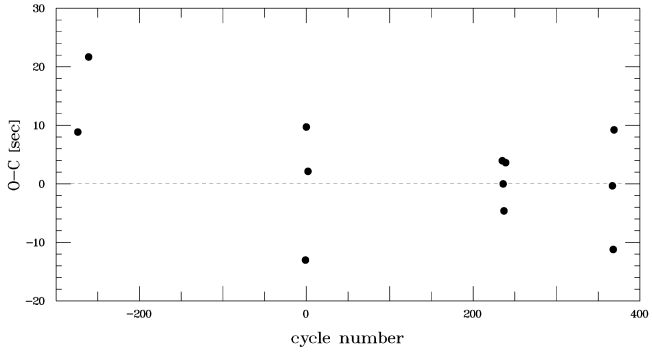

FIG. 1.—$O-C$ diagram of eclipse timings

TABLE 1

JOURNAL OF OBSERVATIONS

Date (1999)	Start (UT)	End (UT)	Time Resolution (s)	Number of Integrations	Passband
			Photometry		
May 4	05:32	07:22	69	98	V
May 5	05:18	06:41	31	180	R
May 9	00:54	06:42	5	1463	...
May 24/25	23:35	07:43	3	8682	...
May 31/June 1.....	23:20	07:06	124	198	J
June 1/2	22:34	07:19	35	887	H
June 11/12	22:32	06:28	3	6435	$CuSO_4$
June 21/22	22:39	06:12	3	5291	...
			Spectroscopy		
June 2	02:23	03:33	300	2	...

NOTE.—Start and end times are in hours and minutes.

TABLE 2

ECLIPSE EPOCHS

Date	Eclipse Number	HJD (2,451,000+)
1999 May 4	−274	302.79523
1999 May 5	−261	303.78289
1999 May 25.....	−1	323.53261
	0	323.60879
	2	323.76063
1999 Jun 11	235	341.45976
1999 Jun 12	236	341.53568
	237	341.61158
	239	341.76360
1999 Jun 21	367	351.48667
1999 Jun 22	368	351.56251
	369	351.63871

Therefore, the minimum phase will be slightly offset from the phase of conjunction of the red and the white dwarf.

We measured the epochs of the eclipse minima in two ways: (1) by fitting a high-order polynomial to the eclipse bottom and calculating the location of its minimum; (2) by fitting straight lines to the linear parts of the ingress and egress and calculating the epoch of the intersection of these lines. In some cases sudden changes in the slope of the ingress or egress can be discerned. Those parts of the light curves closer to the minimum were then used. Both methods gave largely consistent results: The mean of the differences of the minimum epochs (in the sense method 1 minus method 2) is 5.9 $\pm$ 9.8 s. The means of the two epochs determined for each eclipse are listed in Table 2.

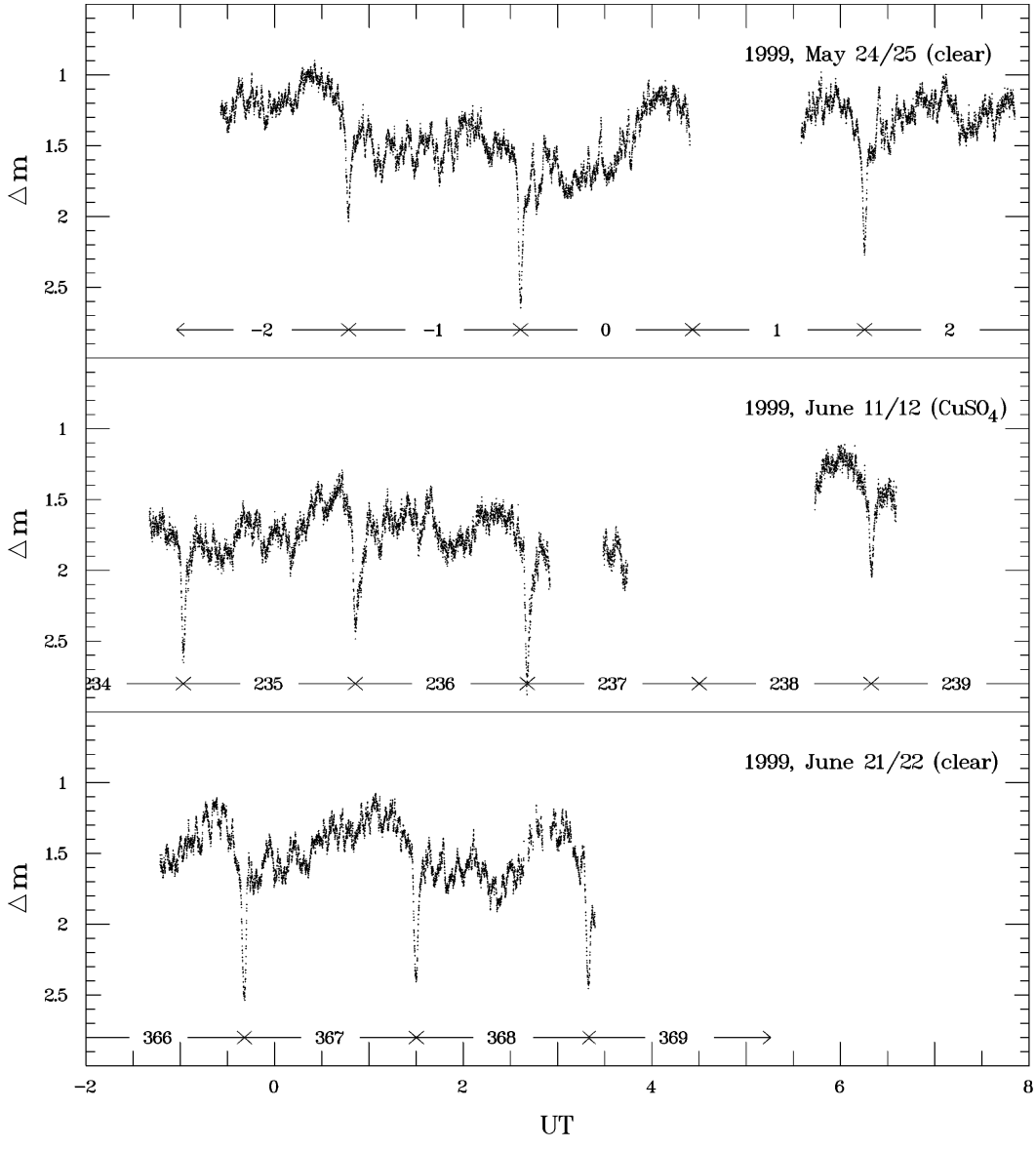

FIG. 2.—Light curves of V893 Sco

The epochs of the eclipses observed in the low-resolution light curves of May 4 and 5 could not be obtained in this way. They were simply estimated by a visual inspection of the light curves and are thus less accurate. Therefore, they were not used to calculate the ephemeris. But they were useful to make sure that no cycle count ambiguities occurred.

A linear least-squares fit to the remaining eclipse timings yields the following ephemeris:

$$\begin{aligned}\mathrm{HJD(min)} = {} & 2{,}451{,}323.60868(\pm 0.00003) \\ & + 0.07596185(\pm 0.00000012)E\ .\end{aligned}$$

An $O-C$ diagram of the difference between observed and calculated eclipse epochs (also including the eclipses of May 4 and 5) is shown in Figure 1. This photometric period is in agreement with the (much less accurate) spectroscopic period favored by Thorstensen (1999).

4. THE LIGHT CURVES

4.1. The Optical Range

4.1.1. General Characterization

The light curves of V893 Sco exhibit deep eclipses recurring at intervals of 01:49:23 (see § 3), strong flickering, and during most orbits, a well-developed hump preceding the eclipse. In these respects the behavior of V893 Sco is very reminiscent of prototypical eclipsing dwarf novae of the SU UMa subtype such as OY Car (Wood et al. 1989) or Z Cha (Wood et al. 1986). The high-resolution optical light curves of May 24/25, June 11/12, and June 21/22 are shown in Figure 2 (the observations of May 9 are not shown because they contain many gaps due to intermittent clouds). In order to facilitate the subsequent discussion, the cycle numbers according to the ephemeris derived in § 3 are shown below the light curves (the cycle number is taken to be equal to the number of the eclipse occurring at the *beginning* of the cycle).

In spite of the similarities with high-inclination SU UMa stars, V893 Sco exhibits some peculiarities which are not observed—at least not to this extent—in those systems. The properties of V893 Sco are less stable in the following aspects:

1. The overall light level of V893 Sco can vary substantially from one orbit to the next. Regard, e.g., the brightness during the first half of the orbit (i.e., before the orbital hump) on May 24/25. It declines by about 0.5 mag from cycle -2 to cycle 0 and rises by the same amount during cycle 2. A similar brightening happened during cycle 238 on June 11/12.

2. There are significant differences of the minimum magnitude as well as of the eclipse amplitude. We searched for correlations between eclipse depth, minimum magnitude, magnitude level before or after eclipse, and hump amplitude. No significant correlation between these parameters exists in our data.

3. The orbital hump exhibits strong variations. It can be very well developed—e.g., in cycle 0, cycle 1, and all cycles observed on June 21/22—or almost absent as during cycle -1. There is no smooth transition between these states as is evident from the difference between cycles -1 and 0. Moreover, from time to time V893 Sco appears to develop during the first part of the orbit a so-called intermediate hump as sometimes observed, e.g., in OY Car (Schoembs & Hartmann 1983) and in particular in WZ Sge (Patterson 1980; R. E. Nather 1992, private communication). Examples are cycles 2 and 236.

4.1.2. The Eclipses

A synopsis of the individual eclipses is shown in Figure 3. The eclipse shape is by no means constant but exhibits substantial variations from cycle to cycle. The ingress is in general smooth without a noticeable step or change of gradient at an intermediate level which is characteristic for some other short-period dwarf novae such as Z Cha (Cook & Warner 1984) and OY Car (Vogt et al. 1981), where these features separate the eclipse ingress of the white dwarf and the hot spot, respectively. The exception is eclipse E$-$1, which clearly shows a step. However, since it is absent in all other eclipses we presume that it is due to some flickering activity still visible at that phase.

The eclipse egress appears to be more variable than the ingress. At times the system brightness at the end of the egress is about the same as that at the start of the ingress (e.g., E367), while at other times the system is much fainter at the end of egress than before the eclipse (e.g., E236). Together with the quite variable amplitudes and minimum levels of the eclipses seen in Figure 2, this tells us that the eclipsed body itself is quite variable. We have already mentioned that the orbital hump varies a lot in strength. Moreover, the total eclipse width is only ≈ 0.035 in phase. This is much shorter than in most other eclipsing CVs, where the corresponding value is typically of the order of 0.1, suggesting a grazing instead of a total eclipse in V893 Sco. All this evidence points at the hot spot (together with a part of the accretion disk) as being the eclipsed body, while the center of the disk together with the white dwarf remains uneclipsed.

The latter conclusion is supported by the eclipse amplitude. We measured the magnitude difference between eclipse minimum and the mean brightness in the phase interval $0.2 \leq \phi \leq 0.4$. In an idealized picture we would see only the undisturbed accretion disk and the white dwarf at these phases. In reality some residual light of the hot spot

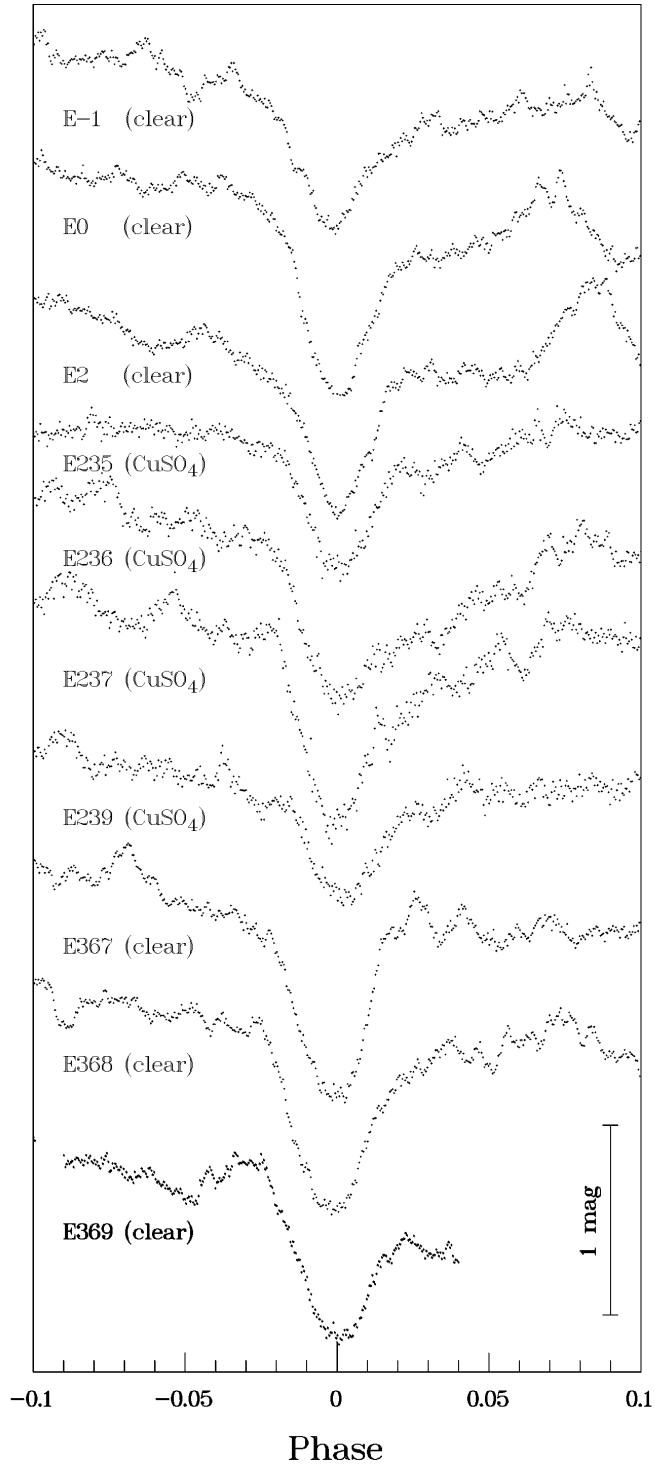

FIG. 3.—Synopsis of the individual eclipses observed in V893 Sco

might still be visible, and occasionally the light source responsible for the intermediate hump also contributes. Thus, these amplitudes are upper limits to what would be measured if we would see nothing but the accretion disk in the quoted phase range. Nevertheless, the measured amplitude is often less than 0.75 mag, meaning that during minimum less than half of the disk light is eclipsed. Thus, the white dwarf remains visible at minimum. Note that this will unfortunately hinder studies of the accretion disk structure in V893 Sco with eclipse mapping techniques.

While we are convinced that the eclipses are mainly due to the hot spot, some details of the observations are still to be explained. Naively we would expect a correlation between the hump amplitude and the eclipse depth. However, this is not observed. But then, it is not easy to measure the hump amplitude reliably in view of the strong cycle-to-cycle variations of the mean system brightness and the occasional presence of the intermediate hump. Moreover, we cannot be confident that the hot spot eclipse is (always) total. It is not guaranteed that the (three-dimensional) shape of the hot spot is constant. Various degrees of eclipse of the hot spot would also naturally explain the strong differences of the residual magnitude of V893 Sco during eclipse minimum.

The eclipse ingress in V893 Sco takes longer than the egress. This is in contrast to other eclipsing CVs, where the egress is in general more gradual than the ingress because in a combined disk/white dwarf and hot spot eclipse the hot spot enters into eclipse and reemerges later than the bright central parts of the accretion disk. However, if the eclipse is essentially only due to the hot spot, an elongated spot shape, seen much more foreshortened during egress than ingress, can cause the egress to be more rapid than the ingress. Thus, the unusual sense of the eclipse asymmetry is another argument indicating that the eclipsed body is essentially the hot spot.

4.1.3. The Orbital Inclination

Knowing that the accretion disk eclipse is partial but that the disk center remains always visible can help to put constrains on the orbital inclination i of V893 Sco. Accounting for the shape of the secondary assuming Roche geometry as approximated by Kopal (1959), we calculated an upper limit for i as a function of the mass ratio $q = M_2/M_1$. This is the upper graph in Figure 4. In order to get a lower limit for i, we assume the disk to have a radius of $0.35a$, where a is the component separation. This is a typical value found in several other systems (see Bruch 1992 for references of relevant measurements). Grazing disk eclipses then occur at inclinations as shown by the lower graph in Figure 4. Since the disk eclipse could be anything between grazing and just missing white dwarf eclipses, its width is not helpful to put further constrains on i and q.

4.1.4. Oscillations

In order to check if a coherent oscillation hides in the flickering, we calculated Lomb-Scargle periodograms (Lomb 1976; Scargle 1982; Horne & Baliunas 1986) of the

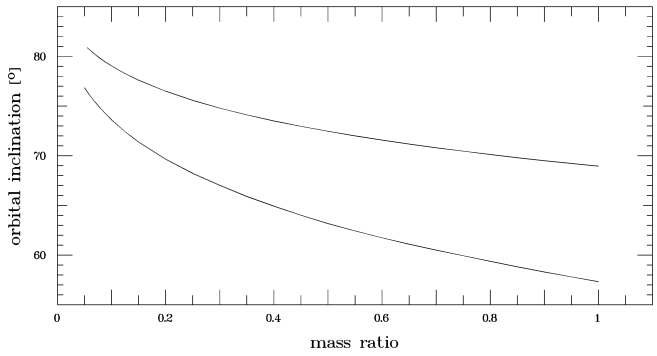

FIG. 4.—Upper and lower limits for the orbital inclination of V893 Sco as a function of the mass ratio.

light curves. In order to reduce the low-frequency signals introduced by the orbital modulations, the eclipses were first cut out, and a spline fit to a binned version of the light curves (bin width 15 minutes) was subtracted.

A significant signal leading to a convincing curve when folding the light curve on the corresponding period was found on 1999 June 21/22. The periodogram is shown in the upper frame of Figure 5. The peak at $2.92 \pm 0.01 \times 10^{-3}$ Hz suggests a period of $P_{\rm osc} = 5.71 \pm 0.02$ minutes. The light curve, folded on this period, is shown in the central frame of Figure 5. Although the random flickering dominates the curve exhibits definitely a sinusoidal modulation. This is better seen in the lower frame of Figure 5 which contains a binned version (bin width $0.01 \times P_{\rm osc}$) of the light curve in the central frame. The solid line represents the best-fit sine curve which has a half-amplitude of 0.0319 ± 0.0007 mag.

The light curves of the other nights do not exhibit a signal at the corresponding frequency (or a convincing modulation at other frequencies). Only the periodogram of 1999 May 9 contains a conspicuous peak (although much less significant than on 1999 June 21) at a nearby frequency of $2.72 \pm 0.01 \times 10^{-3}$ Hz. Folding the light curve on the corresponding period (6.14 ± 0.02 minutes) results in a curve with a narrow minimum and a double-peaked maximum, i.e., far less sinusoidal than in the previous case. However, the total amplitude of the variations is similar in the two nights.

The periodogram of the combined data of the four nights of high-speed photometry, shown in the insert in the upper frame of Figure 5, contains two maxima—each one consisting of many alias peaks—close the frequencies of the signals found on May 9 and June 21/22, but slightly shifted to higher and lower frequencies, respectively. The distance between the centroids of these maxima corresponds well to the orbital frequency of V893 Sco, suggesting them to be a periodic signal and its beat frequency with the orbital cycle.

The modulations discussed above are reminiscent of the variations seen in intermediate polars, although the present observations do not permit to regard them as stable oscillations of V893 Sco. However, their presence is intriguing, and future observations should be scrutinized for similar signals.

4.2. The Near-Infrared Range

We have observed V893 Sco in the J and H bands in the hope to see ellipsoidal variations of the red dwarf. However, in both bands the light curves are essentially constant with a scatter of the data points of $\sigma_J = 0.024$ mag and $\sigma_H = 0.073$ mag (see Fig. 6).

In order to verify if this nondetection can be explained by dilution of the light of the secondary by the primary, we first calculated synthetic J and H light curves of the secondary alone, employing the Wilson-Devinney code (Wilson & Devinney 1971; Wilson 1979) in mode 5 (secondary star filling Roche lobe). The well-known relation between the mass M_2 and the radius R_2 of the secondary star in CVs, and the orbital period (as can be derived from the expression for the ratio of R_2 and the component separation a as a function of the mass ratio q [Paczyński 1971] and Kepler's law), together with the mass-radius relation for late-type main-sequence stars as calibrated by Caillaut & Patterson (1990), leads to $R_2 = 0.18\ R_\odot$ and $M_2 = 0.144\ M_\odot$. Assuming the white dwarf to a have a mass similar to that of the peak of the overall white dwarf population, we get a mass ratio $q \approx 0.25$. For the orbital period we take $i = 71\overset{\circ}{.}9$; i.e., the mean of the upper and lower limits (Fig. 4) at $q = 0.25$. A gravity-darkening exponent of 0.32 (Lucy 1967) was assumed. Since the limb-darkening coefficient for very cool stars in the near-IR is not well known, we adopted an arbitrary but reasonable value of 0.8. In order to estimate the temperature, we used the theoretical mass-luminosity relation of Neece (1984) (for consistency because the secondary-star mass was calculated from relations given by Caillaut & Patterson 1990, who also employed the relation of Neece) to calculate the luminosity which together with the radius of $R_2 = 0.18\ R_\odot$ yields a temperature of $T_2 = 2640$ K, assuming blackbody radiation. As a consistency check we constructed a mass–spectral type relation, restricting ourselves to the few main-sequence stars for which good mass determinations are possible: YY Gem (M1 V; 0.62 and 0.57 $M_\odot$; Leung & Schneider 1978), GJ 2069A (M3.5 V; 0.433 and 0.397 $M_\odot$; Delfosse et al. 1999), CM Dra (M4.5 V; 0.231 and 0.214 $M_\odot$; Lacy 1977; Metcalfe et al. 1996) and RR Cae ($\approx$M6.5 V; 0.095 $M_\odot$; Bruch 1999a). This relation suggests a spectral type of $\approx$M5.8 for the V893 Sco secondary. Finally, a spectral type–temperature relation constructed by Bruch (1999b) from results of model fits to the spectra of late type dwarfs of Leggett et al. (1996) yields $T_2 = 2840$ K. In view of the numerous uncertainties involved we consider the two tem-

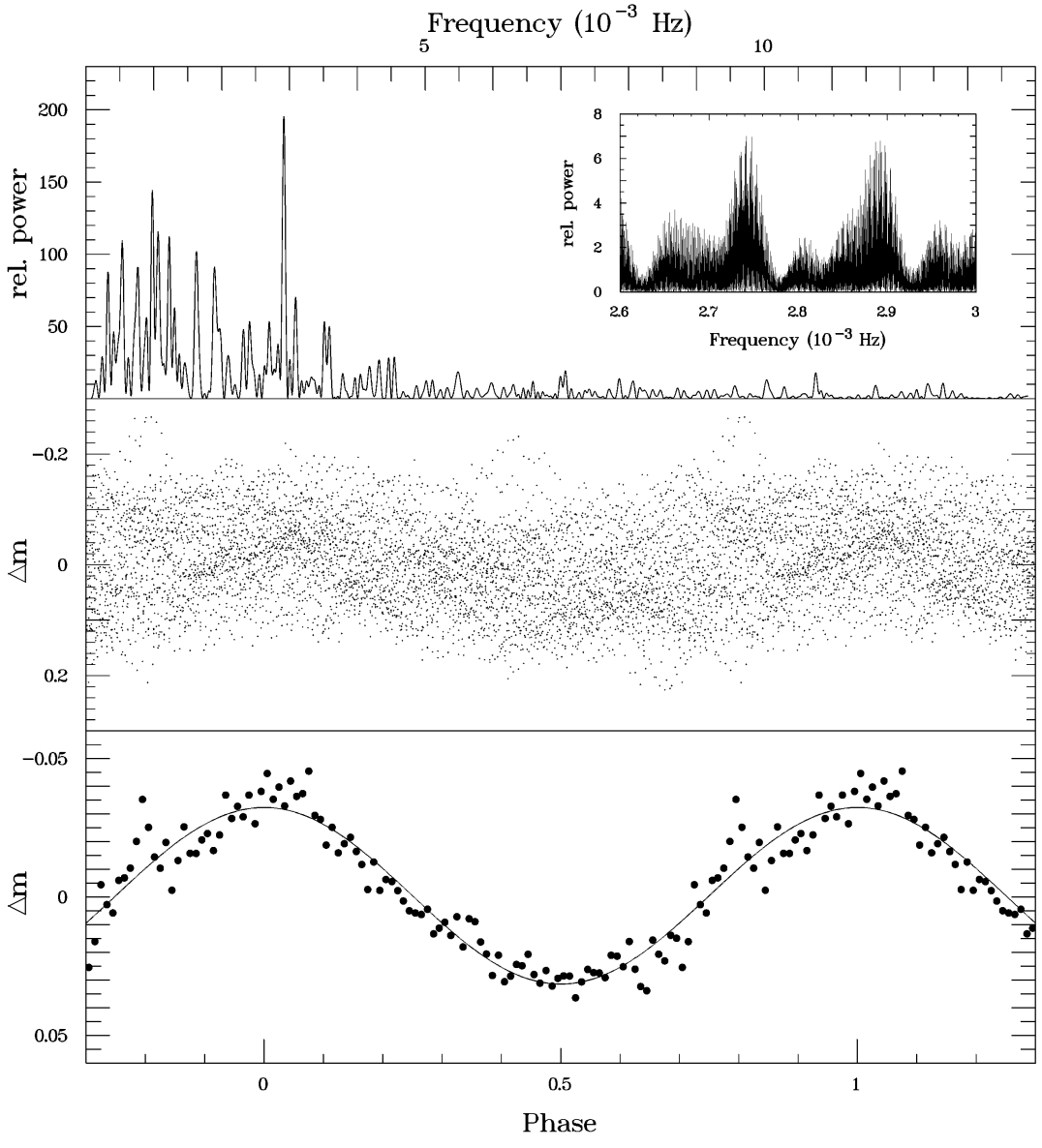

FIG. 5.—*Top:* Lomb-Scargle periodogram of the light curve of 1999 June 21/22. The insert contains a section of the periodogram of the combined data of all four nights of high-speed photometry. *Middle:* Light curve (after removing eclipses and variations on timescales longer than 15 minutes) folded on $P_{osc} = 5.709$ minutes. *Bottom:* Same as above, but binned in phase bins of width $0.01 P_{osc}$; the solid line is the best-fit sine curve.

perature values consistent. For the sake of more conservative limits we adopt the higher one hereafter.

The resulting secondary light curves have total amplitudes of 0.38 mag in J and 0.36 mag in H. This should be easily visible in the combined system light curves were it not for the dilution by the light from the primary. To estimate this contribution a steady state disk spectrum was calculated, approximating the disk as rings of blackbodies with temperatures depending on their distance from the center. Although the disk of a quiescent dwarf nova may not be in a steady state, this approach is justified for an order-of-magnitude estimate. Assuming a mass accretion rate of $5 \times 10^{-10}\ M_\odot\ \mathrm{yr}^{-1}$, $M_1 = 0.58\ M_\odot$, an inner disk radius corresponding to the radius of a white dwarf of this mass, and an outer radius of 0.35 times the component separation (see § 4.1.3), we calculated the total energy radiated by the disk into the unit solid angle per time and wavelength unit at the central wavelengths of the J and H bands. This was compared to the corresponding values calculated for the secondary, adopting a temperature and radius as quoted above.

It was found that the disk was 42 and 23 times brighter than the secondary in the J and H bands, respectively. The amplitude of the ellipsoidal variations of the late-type star

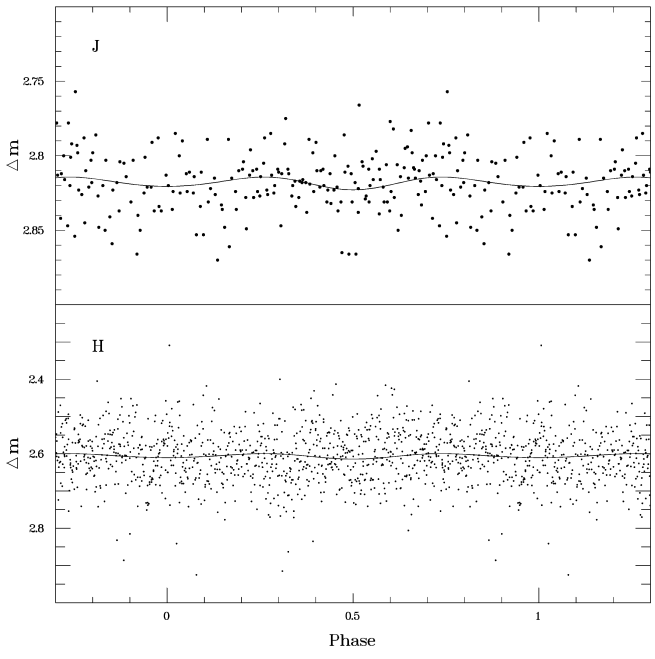

FIG. 6.—Orbital light curves in the near-infrared J and H bands (*dots*). The solid lines show the predicted ellipsoidal variations of the secondary star, based on model calculations, diluted by the light of the primary component. The scatter of the data points is clearly too large to distinguish these variations in the observations.

would be reduced to 0.0085 mag (J) and 0.015 mag (H) in the combined light. This would remain undetectable as is illustrated in Figure 6 where the two frames show the observed J and H light curves (*dots*) together with the calculated ones (*solid lines*) as a function of phase. This conclusion remains valid even if the adopted system parameters are varied substantially (within reasonable limits). The strongest effect can be caused by the mass accretion rate $\dot{M}$; but even modifying $\dot{M}$ by a factor of 10 changes the radiation emitted by the disk by no more than a factor of ≈ 2 at J and H.

While the absence of detectable ellipsoidal variations in the light curves can thus be explained, the complete absence of any trace of an eclipse is more vexing. The hump amplitude in the white light curves is of the order of 0.4 mag which translates into a ratio between disk and hot spot flux of $F_D/F_{HS} = 0.45$. Assuming 5500 Å to be the isophotal wavelength corresponding to the "white light transmission function" and the spectral energy distribution of V893 Sco, we can calculate the expected flux ratio for the disk (using the same model parameters as above) and the hot spot between the optical and the J and H bands, respectively. The hot spot is assumed to radiate like a blackbody of 12,000 K, a temperature typically observed in many systems (Marsh 1988; Robinson, Nather, & Patterson 1978; Schoembs & Hartmann 1983; Wood et al. 1986, 1989; Zhang & Robinson 1987). In both infrared bands a flux ratio of $F_D/F_{HS} \approx 0.60$ would then be expected, a value which is rather independent of the hot spot temperature because in the IR bands we see basically the Rayleigh-Jeans tails of the spectral energy distribution of both the disk and the hot spot. Thus, an eclipse not much less deep as in visual light would be expected. We cannot explain why we do not see this in our observations.

5. THE SPECTRUM

Our two optical spectra of V893 Sco between 4650 and 5540 Å were taken close together in phase. Therefore, we summed them in order to increase the signal-to-noise ratio and display the results, normalized to the continuum, in Figure 7.

The only obvious spectral line in the observed range is Hβ (the helium lines clearly seen in the spectrum of Thorstensen 1999 are almost drowned in the noise). The structure of the Hβ emission is typical for dwarf novae with a high orbital inclination. It consists of two peaks separated by a minimum. This is the signature of emission from an accretion disk seen more or less edge-on (see, e.g., Horne & Marsh 1986). The red peak is significantly brighter than the blue one. This can be explained as being due to an S-wave caused by the hot spot as seen in the trailed spectra of many dwarf novae (e.g., Honeycutt, Kaitchuck, & Schlegel 1987).

The present spectrum was obtained at orbital phase 0.84. Close to this phase all systems with an obvious S-wave in the atlas of Honeycutt et al. (1987) exhibit the maximum redward excursion of the wave. Its superposition with the usual accretion disk double peak will then result in a particularly strong red peak, as observed. The line profile in Figure 7 thus permits to predict that V893 Sco will show a strong S-wave in time-resolved spectra.

This is confirmed by the more encompassing spectroscopic observations of Thorstensen (1999). Phase-folding his radial velocity measurements using our more accurate ephemeris yields a radial velocity curve which shows a

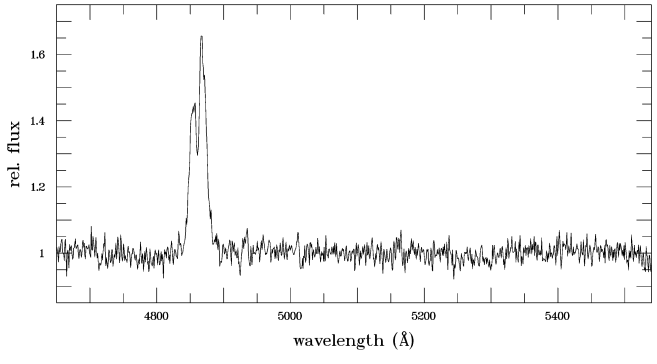

FIG. 7.—Spectrum of V893 Sco in the region around Hβ, normalized to the continuum.

maximum recession velocity (as defined by a least-squares sine fit) at phase −0.135 with respect to the eclipse minimum. This is in stark contrast to what is expected if the emission comes from the accretion disk, but is in accordance with the expected velocity phasing of the stream of matter transferred from the secondary, seen approximately tangentially at phase −0.135. The absolute value of the velocity, however, is much less than the free fall velocity near the outer disk rim. Thus, it appears plausible that the emission comes from the matter transferred from the secondary, decelerated in the hot spot but still retaining the original direction of velocity.

It therefore seems that in spite of Thorstensen's efforts to measure the line wings the radial velocities are still dominated by the hot spot emission. In consequence, any attempt to derive masses from these data is doomed, emphasizing again that dynamical properties of CVs—except for the orbital period—depending on such emission-line radial velocities are notoriously unreliable.

The separation of the peaks of Hβ in our spectra is $\approx$820 km s^{-1}, somewhat smaller than the separation measured by Thorstensen (1999) in the helium lines ($\approx$1200 km s^{-1}). This is consistent with the idea that the hydrogen emission arises preferentially farther out in the accretion disk than the helium emission.

6. THE FLICKERING ACTIVITY

6.1. Wavelet Analysis

The light curve of V893 Sco exhibits the strong flickering activity typical for cataclysmic variables. In order to quantify these stochastic variations, a wavelet analysis following the guidelines of Fritz & Bruch (1998) was performed. Since wavelet techniques are not yet widely applied in the analysis of light curves, we give a short summary here.

The wavelet transform (see Jawerth & Sweldens 1994; Chui 1992; and Scargle et al. 1993 for general introductions and applications to stochastic data) permits the decomposition of a signal according to a localized function, the (finite) carrier of which is tied to the investigated scale. The base functions—the wavelets—are scaled versions of a fundamental function, the mother wavelet. The wavelet transform of a time-dependent signal is then a representation of the signal in time *and* frequency.

To a certain degree the shape of the mother wavelet can be adjusted to the signal. Studying the flickering in CVs, a wavelet with a triangular shape matches the individual flares in the light curve well, making a wavelet analysis superior to a classical Fourier analysis which uses sinusoids as base functions. Flickering is a stochastic signal. Therefore, it is not important to know exactly when a particular event (a flare) occurs. Instead, the distribution of the strength of the variations among different timescales is of interest. Scargle et al. (1993) introduced the scalegram for the study of such data. It measures basically the variance of the wavelet coefficients as a function of the timescale. A suitable normalization defined by Fritz & Bruch (1998) then permits a direct comparison obtained from light curves observed under different conditions: The normalized scalegram describes the variance of the modulated part of the light curve in units of the square of all data points.

Fritz & Bruch (1998) found the coiflet C12 (Daubechies 1992) to be the most suitable for the analysis of flickering data. Using this mother wavelet we calculated scalegrams for all our high time resolution light curves of V893 Sco. Figure 8 shows the normalized scalegrams after 200 bootstrap replications (Efron & Tibshirani 1993), accounting for the fact that the points in a flickering light curve are not statistically independent (Fritz & Bruch 1998). The scalegrams are remarkably similar concerning their slope as well as their vertical location in the double-logarithmic diagram.

Due to the linear rise of the scalegram, its essence can be condensed into two parameters, the slope α of a straight line fitted to the scalegram points, and $\Sigma = \log S(t_{\rm ref})$, where S is the scalegram value and $t_{\rm ref}$ is a reference timescale (for details, see Fritz & Bruch 1998). The term α measures the distribution of the strength of the flickering among different timescales. In all CV light curves $\alpha > 0$ because the flickering on long times scales is stronger than on short ones. However, the larger $|\alpha|$ is, the more the flickering on long times scales dominates over that on short ones. Σ measures the overall strength of the flickering with respect to the unmodulated background light.

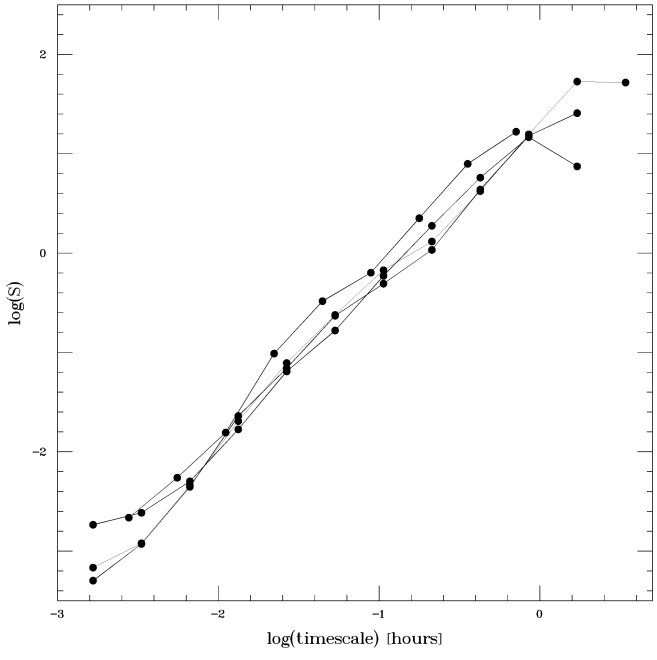

FIG. 8.—Scalegrams of the light curves of V893 Sco in four nights

Using the same weighting scheme as Fritz & Bruch (1998), as well as their reference timescale $t_{ref} = 3$ minutes, we determined the scalegram parameters for V893 Sco as listed in Table 3. Comparing these values with the location of other quiescent SS Cyg and SU UMa stars in the α-Σ diagrams of Fritz & Bruch (1998), we see that V893 Sco occupies the upper right part of the distribution, indicating a rather strong flickering with respect to the unmodulated light along with a steep distribution which means that the flares on longer times scales dominate strongly over those on shorter scales. However, more remarkable is the good repeatability of the flickering properties from one night to the next. Whereas the scalegram parameters of a given dwarf nova in general scatter over quite a large range in the α-Σ diagrams (see Fritz & Bruch 1998), they are constrained to a very narrow range in the case of V893 Sco. This is reminiscent of what Fritz & Bruch (1998) found for the intermediate polars.

6.2. The Location of the Flickering Light Source

The question where in a CV the flickering arises is still pending. An early answer for the case of the prototypical dwarf nova U Gem was expressed by Warner & Nather (1971): They assume the flickering to be due to modulations of the hot spot caused by variations in the mass transfer from the secondary. However, there is ample evidence that this cannot be the only source of flickering in CVs in general. Many observations throughout the literature indicate that the bulk of the flickering arises in the inner accretion disk or on the white dwarf (see Bruch 1992 for a list of references). Moreover, Bruch (1992) showed that the energy released by the flickering cannot be drawn from the impact of matter transferred from the secondary onto the accretion disk.

Few attempts have been undertaken to actually measure where in a CV the flickering arises. Eclipsing systems are particularly well suited for this purpose. Horne & Stiening (1985) and later Bennie, Hilditch, & Horne (1996) performed a corresponding study of RW Tri, while Welsh & Wood (1995) and Welsh, Wood, & Horne (1996) did the same for HT Cas. In each case the origin of the flickering in the inner disk was confirmed.

TABLE 3

PARAMETERS OF THE FLICKERING OF V893 SCO

Date	α	Σ
1999 May 9	1.74 ± 0.05	-0.52 ± 0.10
1999 May 25.....	1.63 ± 0.03	-0.76 ± 0.05
1999 June 11.....	1.70 ± 0.01	-0.78 ± 0.02
1999 June 21.....	1.61 ± 0.03	-0.78 ± 0.06

The most extensive investigation of this kind was performed by Bruch (1996), who analyzed light curves of Z Cha in quiescence, normal eruptions, and superoutbursts. Again, it was found that the bulk of the flickering comes from close to the white dwarf. However, Bruch (1996) also showed that a minor but not insignificant part of the low-amplitude, small-timescale flickering arises in the hot spot.

We applied the technique developed by Bruch (1996) to V893 Sco: Carefully smoothed light curves were subtracted from the original ones which were expressed in terms of photons detected by the CCD. The scatter of the residual curves is basically due to flickering and photon (Poisson) noise. Other noise sources such as scintillation and readout noise are negligible. The sky background was included in the count rates since it contributes to the Poisson noise, but is also insignificant. The standard deviations of the data within small intervals of the difference curves, after correcting for the photon noise, is then a measure for the strength of the flickering in these intervals. The final rms scatter curve as a function of orbital phase was composed by applying the above method to as many cycles as possible, normalizing the individual curves, and then taking the mean of the standard deviations in a given phase interval. For more details about the technique, see Bruch (1996).

The basic difference between this method and that used by the other authors listed above is that we determined the rms scatter as a function of phase for each light curve individually and then take the mean over many cycles, whereas they take the mean of their orbital light curves (trying to account for long-term variations) and only then calculate the rms scatter. A critical comparison of the two methods will be published elsewhere (A. Bruch 2000, in preparation).

We adopted the same parameters as Bruch (1996) in the case of Z Cha when we smoothed the original light curve. This means in particular that the method is only sensitive to flickering on timescales below 0.01 cycles (about 1.1 minutes in the present case). The resulting mean rms scatter curve, normalized to a mean value of 1, is shown in the upper frame of Figure 9. The scatter was calculated in phase intervals of $\Delta\phi = 0.0025$, but the step width between intervals is only half that value. Thus, neighboring points are not independent of each other. A representative error bar is drawn in the lower left corner. However, since the statistical error is not constant (in particular decreasing during eclipse), the lower frame of Figure 9 contains the standard deviation of the mean rms values as a function of phase (note that both diagrams are drawn on the same scale).

Two important properties of the rms scatter curve are immediately obvious: During the eclipse it drops to a minimum, and there is a noticeable maximum during the second half of the cycle, coincident with the orbital hump. The presence of the latter indicates that a part of the flickering in V893 Sco has its origin in the hot spot, just as in Z Cha during quiescence.

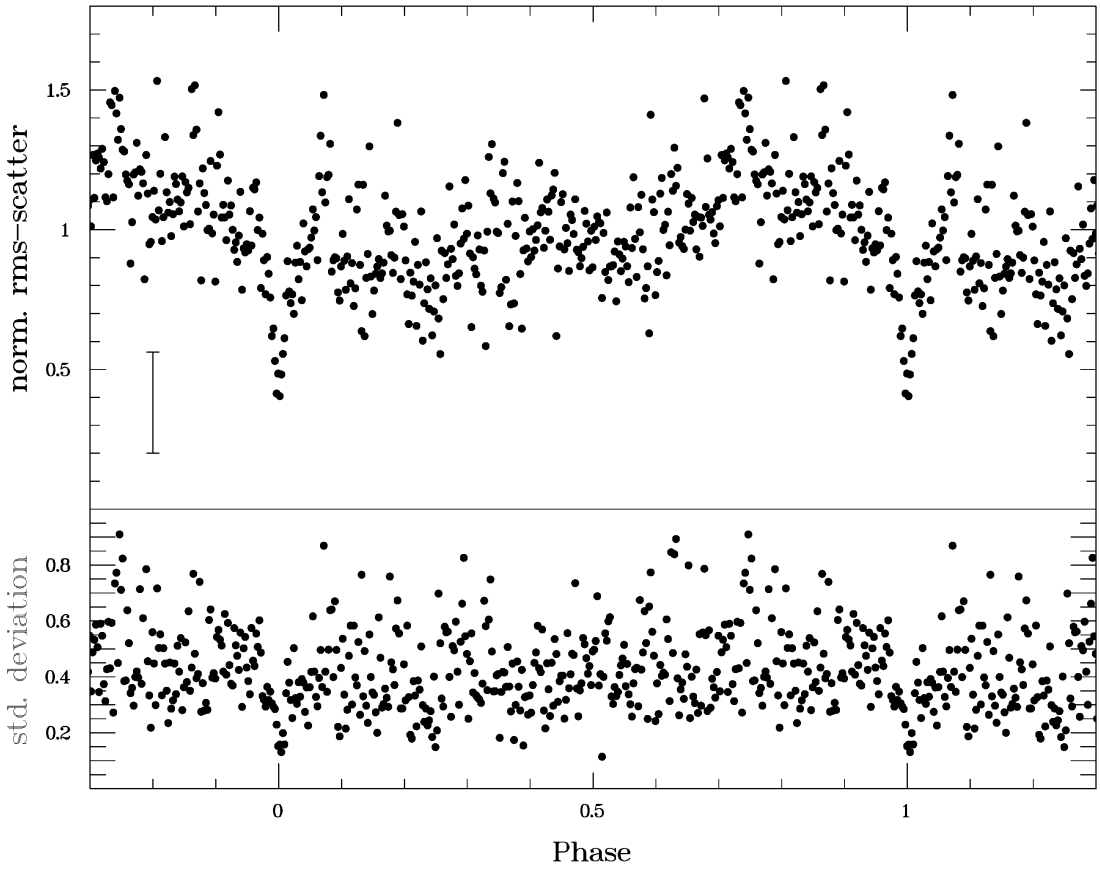

FIG. 9.—*Top*: The rms scatter in the light curves of V893 Sco as a function of orbital phase. *Bottom*: Standard deviation of the rms scatter.

The behavior of the rms scatter curve during eclipse is better seen in Figure 10 where the upper and lower frames, respectively, show the mean eclipse profile of V 893 Sco and the rms scatter on an expanded scale. The dashed vertical lines indicate the phases of first and last eclipse contact as defined visually in the mean eclipse. The V-shape of the rms eclipse suggests that the flickering light source is never totally out of view. At first glance the fact that is does not reach down to zero suggests the same. However, this may be misleading because the light curve may contain residual noise which is not accounted for by the method used to calculate the rms scatter curve (Bruch 1996).

Assuming that the hot spot eclipse is total we can make a statement about the relative strength of the flickering arising in the hot spot and that part of the flickering which occurs in the eclipsed part of the accretion disk. For this purpose we define three phase ranges as $R_1 \equiv -0.3 \leq \phi \leq -0.1$ (orbital hump), $R_2 \equiv -0.005 \leq \phi \leq 0.005$ (eclipse bottom), and $R_3 \equiv 0.1 \leq \phi \leq 0.5$ (accretion disk; no contribution of hot spot). Let σ_o be the observed rms scatter, $\sigma_{f_{HS}}$ the scatter due to the hot spot flickering, and $\sigma_{f_{D,e}}$ and $\sigma_{f_{D,u}}$ the scatter due to the disk flickering originating in the eclipsed and uneclipsed parts of the disk, respectively. Finally, σ_r is the scatter due to any residual noise sources

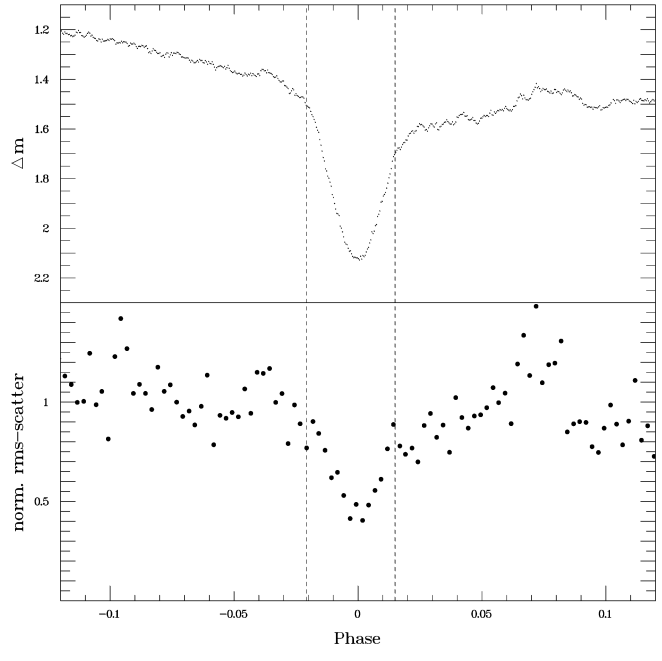

FIG. 10.—*Top*: Mean eclipse of V893 Sco. *Bottom*: Expanded view of the rms scatter curve during eclipse.

which might be present (see Bruch 1996). Then

$$\sigma_o^2(R_1) = \sigma_r^2 + \sigma_{f_{D,u}}^2 + \sigma_{f_{D,e}}^2 + \sigma_{HS}^2 ,$$
$$\sigma_o^2(R_2) = \sigma_r^2 + \sigma_{f_{D,u}}^2 ,$$
$$\sigma_o^2(R_3) = \sigma_r^2 + \sigma_{f_{D,u}}^2 + \sigma_{f_{D,e}}^2 .$$

Inserting the values of σ_o measured in the rms scatter curve leads to a ratio $\sigma_{f_{D,e}}/\sigma_{f_{HS}} = 0.75 \pm 0.31$. Assuming for an order-of-magnitude estimate that the true ratio between white dwarf/disk flickering and hot spot flickering is 1.3 as in Z Cha (Bruch 1996) and that the rms scatter due to the eclipsed and uneclipsed disk flickering add quadratically to the variance due to the total disk flickering, we find a ratio $\sigma_{f_{D,u}}/\sigma_{f_{D,e}} = 1.4$. If the flickering were distributed homogeneously across the entire disk this should also be the ratio of the areas of the uneclipsed and eclipsed parts of the disk. Since all studies performed so far indicate that the flickering is concentrated toward the inner disk, this value can be regarded as an upper limit to the true ratio.

In order to test if the statistical properties of the flickering during phases of visibility of the hot spot and at other phases are systematically different, we calculated separately wavelet transforms of those parts of the light curves which contain a prominent hump and other parts without an orbital hump (or intermediate hump). Note that the wavelet technique samples the flickering on all timescales, not just the small ones. No systematic differences were found. This can be interpreted in two ways: (1) The statistical properties of hot spot and disk flickering are similar. However, in view of the different physical mechanisms which must probably be invoked to explain the two types of flickering this appear implausible. (2) Disk flickering dominates strongly over hot spot flickering on long timescales, making up for the hot spot contribution on small ones. We favor the latter interpretation.

7. DISCUSSION AND CONCLUSIONS

In many respects V893 Sco behaves like a typical dwarf nova. However, it exhibits also some peculiarities. Our observations show a strong orbital hump as seen in many other high-inclination systems, in particular the low-period ones. Its presence indicates that the accretion disk is comparatively faint, suggesting nonstationary conditions during quiescence as is typically assumed for dwarf novae. But cycle-to-cycle variations of the strength of the hump were rarely observed to be as marked as in V893 Sco: HT Cas (Patterson 1981) and V4140 Sgr (Baptista, Jablonski, & Steiner 1989; R. Baptista 1992, private communication) show such a behavior to a certain degree, but only in V2051 Oph (Warner & Cropper 1983; Warner & O'Donoghue 1987) is the hump variability as strong as in V893 Sco.

V893 Sco exhibits the strong flickering activity typical for CVs. It is even stronger than in most other dwarf novae in quiescence, however, not unprecedented. Its strength and the slope of the scalegram calculated from the wavelet transform are comparable to those of, e.g., HT Cas and V436 Cen (see Fritz & Bruch 1998). But in contrast to most other CVs for which a corresponding analysis has been performed (with the notable exception of some intermediate polars), the location of V893 Sco in the α-Σ plane as defined by Fritz & Bruch (1998) is extremely constant. Since this is the case in spite of the strong variations in the strength of the orbital hump, this is another argument indicating that the bulk of the flickering is not due to the hot spot.

Although the evidence for V893 Sco to be an intermediate polar is far from conclusive and such a classification would be more than premature, we mention that the hard X-rays observed by *ROSAT*, the comparatively strong (for a dwarf nova) He II λ4686 emission seen by Thorstensen (1999), and the observation of an oscillation in the typical range of periods also possibly indicate a connection between V893 Sco and the intermediate polars. However, none of these features is sufficient evidence to imply a magnetic nature of the system.

The X-ray emission from quiescent dwarf novae is expected to arise in an optically thin boundary layer between disk and white dwarf and is observed to be quite hard. V893 Sco conforms to this picture. The X-rays observed in the *ROSAT* All Sky Survey have a hardness ratio $H_1 = 0.94 \pm 0.04$ and $H_2 = 0.53 \pm 0.10$, where $H_1 = (B - A)/(B + A)$ and $H_2 = (D - C)/(D + C)$; A, B, C, D being the count rates in the ranges 0.1–0.4, 0.5–2.0, 0.5–0.9, and 0.9–2.0 keV, respectively. With such high values for H_1 and H_2, V893 Sco ranks among the CVs with the hardest X-ray emission detected by *ROSAT*.

As a dwarf nova below the CV period gap, V893 Sco should either be an ER UMa star (with long superoutbursts and rapidly recurring normal outburst and almost no well-developed quiescent periods), be an SU UMa system (with occasional superoutbursts interspersed among the more common normal outbursts), or belong to the WZ Sge stars (which only exhibit superoutbursts with intervals of the order of years) (Osaki 1996). The light curves published by Satyvoldiev (1982) cover a total time base of about 700 days. They immediately show that V893 Sco cannot be a ER UMa star. The five eruptions which they contain are too much for a WZ Sge star, leaving the identification of V893 Sco as a SU UMa star as the only alternative. To the first order, the recurrence time is about 140 days. Some outburst might have been missed, however, because the light curves contains substantial gaps. One of the best covered parts contains an obvious outburst and what

appears to be the onset of the next one at an interval of about 90 days. But even if this smaller value would be the typical outburst interval, it would still be long compared to the recurrence intervals of other SU UMa stars which is typically of the order of 20–30 days (Szkody & Mattei 1984).

The outburst amplitude estimated from the light curves of Satyvoldiev (1982) is of the order of 2.5 mag. This is well within the range of amplitudes exhibited by other SU UMa stars. Only considering normal outbursts a mean amplitude of 2.9 ± 0.8 mag is derived from the catalog of Bruch & Engel (1994). At maximum V893 Sco reaches $V \approx 11$–11.5. Being located in a region which is frequently scanned for nova outbursts, it is surprising that it has escaped detection (or redetection) for such along time. This also argues for a comparatively long recurrence time of the outbursts.

Finally, the high value of $B-V = 1$ (Petrov & Salvoldiev 1975) is somewhat disturbing. Typical colors of low-period dwarf novae are $B-V \approx 0$ (Bruch & Engel 1994). It is unlikely that interstellar reddening can cause this discrepancy because quiescent dwarf novae, in particular SU UMa stars, are intrinsically quite faint. The bright apparent magnitude of V893 Sco then tells us that it cannot be far away (which is also supported by the large proper motion measured by Thorstensen 1999) and consequently will not be much reddened. Moreover, the continuum slope in the spectra of Thorstensen (1999) clearly shows that V893 Sco is a blue object. If, however, the B measurement of Petrov & Satyvoldiev (1975) has happened to be coincident with an eclipse, the typical eclipse depth of ≈ 1 mag can explain the unusual $B-V$ value perfectly well. Similarly, if the B and V measurements were separated in time by a prolonged interval the strong variations of V893 Sco occurring on orbital timescales may also be responsible for the unusual color measurement.

We thank João Francisco Santos, Jr., for taking the spectra of V893 Sco for us and an anonymous referee for some constructive suggestions. This work was partially supported by a grant of the Conselho Nacional de Desenvolvimento Científico e Tecnológico (301784/95-5).

REFERENCES

Bailey, J. 1979, MNRAS, 187, 645
Baptista, R., Jablonski, F. J., & Steiner, J. E. 1989, MNRAS, 241, 631
Bennie, P. J., Hilditch, R. W., & Horne, K. 1996, in IAU Colloq. 158, Cataclysmic Variables and Related Objects, ed. A. Evans & J. H. Wood (Dordrecht: Kluwer), 33
Bessell, M. S. 1990, PASP, 102, 1181
Bruch, A. 1992, A&A, 266, 237
———. 1993, MIRA: A Reference Guide (Münster: Univ. Münster, Astron. Inst.)
———. 1996, A&A, 312, 97
———. 1999a, AJ, 117, 3031
———. 1999b, A&A, in press
Bruch, A., & Engel, A. 1994, A&AS, 104, 79
Caillaut, J.-P., & Patterson, J. 1990, AJ, 100, 825
Chui, C. K. 1992, An Introduction to Wavelets (San Diego: Academic Press)
Cook, M. C., & Warner, B. 1984, MNRAS, 207, 705
Daubechies, I. 1992, Ten Lectures on Wavelets, CBMS-NSF Series in Applied Mathematics, Vol. 61 (Philadelphia: SIAM)
Delfosse, X., Forveille, T., Mayor, M., Burnet, M., & Perrier, C. 1999, A&A, 341, L63
Efron, B., & Tibshirani, R. J. 1993, An Introduction to the Bootstrap (London: Chapman & Hall)
Fritz, T., & Bruch, A. 1998, A&A, 332, 586
Honeycutt, R. K., Kaitchuck, R. H., & Schlegel, E. M. 1987, ApJS, 65, 451
Horne, J. H., & Baliunas, S. L. 1986, ApJ, 302, 757
Horne, K., & Marsh, T. R. 1986, MNRAS, 218, 761
Horne, K., & Stiening, R. F. 1985, MNRAS, 216, 933
Jawerth, B., & Sweldens, W. 1994, SIAM Rev., 36, 377
Kato, T., Haseda, K., Takamizawa, K., Kazarovets, E. V., & Samus, N. N. 1998, Inf. Bull. Variable Stars, 4585, 1
Kopal, Z. 1959, Close Binary Systems (London: Chapman and Hall)
Lacy, C. H. 1977, ApJ, 218, 444
Leggett, S. K., Allard, F., Berriman, G., Dahn, C. C., & Hauschildt, P. H. 1996, ApJS, 104, 117
Leung, K. C., & Schneider, D. 1978, AJ, 83, 618
Lomb, N. R. 1976, Ap&SS, 39, 447
Lucy, L. B. 1967, Z. Astrophys., 65, 89
Marsh, T. 1988, MNRAS, 231, 1117
Metcalfe, T. S., Mathieu, R. D., & Latham, D. W., Torres G. 1996, ApJ, 456, 356
Neece, G. D. 1984, ApJ, 277, 738
Osaki, Y. 1996, PASP, 108, 39
Paczyński, B. 1971, ARA&A, 9, 183
Patterson, J. 1981, ApJS, 45, 517
———. 1980, ApJ, 241, 235
Petrov, P. P., & Satyvoldiev, V. 1975, Perem. Svezdy Pril., 2, 221
Robinson, E. L., Nather, R. E., & Patterson, J. 1978, ApJ, 219, 168
Satyvoldiev, V. 1972, Astron. Tsirk., 711, 1
———. 1982, Perem. Svezdy Pril., 4, 127
Scargle, J. D. 1982, ApJ, 263, 835
Scargle, J. D., Steiman-Cameron, T. Y., Young, K., Donoho, D. L., Crutchfield, J. P., & Imamura, J. 1993, ApJ, 411, L91
Schoembs, R., & Hartmann, K. 1983, A&A, 128, 37
Szkody, P., & Mattei, J. A. 1984, PASP, 96, 988
Thorstensen, J. R. 1999, Inf. Bull. Variable Stars, 4749, 1
Vogt, N., Schoembs, R., Krzeminski, W., & Pedersen, H. 1981, A&A, 94, L29
Warner, B., & Cropper, M. 1983, MNRAS, 203, 909
Warner, B., & Nather, R. E. 1971, MNRAS, 152, 219
Warner, B., & O'Donoghue, D. 1987, MNRAS, 224, 733
Welsh, W. F., & Wood, J. H. 1995, in IAU Colloq. 151, Flares and Flashes, ed. J. Greiner, H. W. Duerbeck, & R. E. Gershberg (Heidelberg: Springer), 300
Welsh, W. F., Wood, J. H., & Horne, K. 1996, in IAU Colloq. 158, Cataclysmic Variables and Related Objects, ed. A. Evans & J. H. Wood (Dordrecht: Kluwer), 29

Wilson, R. E. 1979, ApJ, 234, 1054
Wilson, R. E., & Devinney, E. J. 1971, ApJ, 166, 605
Wood, J. H., Horne, K., Berriman, G., & Wade, R. A. 1989, ApJ, 341, 974
Wood, J. H., Horne, K., Berriman, G., Wade, R. A., O'Donoghue, D., & Warner, B. 1986, MNRAS, 219, 629
Zhang, E.-H., & Robinson, E. L. 1987, ApJ, 321, 813